J. Phys. D: Appl. Phys. **18** (1985) 1281–1290. Printed in Great Britain

Aggregation of water-based magnetic liquids observed with the polarising microscope

G A Jones
Department of Pure and Applied Physics, University of Salford, Salford M5 4WT, UK

Received 13 July 1984, in final form 11 December 1984

Abstract. Aggregation phenomena in water-based magnetic liquids have been observed using a polarising microscope fitted with a phase compensator. Macrochains formed in an external magnetic field are shown to have a greater birefringence than the surrounding 'unchained' liquid. A simple model of the colloidal suspension allows the optical data to be interpreted and hence a numerical estimate of the birefringence of the macrochains to be made. This indicates that for fluid diluted five-fold, the chain birefringence is some four times greater than the initial bulk birefringence. It is also found that the bulk fluid birefringence remains essentially constant for times up to 2 h, independent of the formation of macrochains.

1. Introduction

It is well known that magnetic liquids exhibit an induced optical anisotropy, e.g. birefringence and dichroism, when exposed to an external magnetic field (Majorana 1902). A further remarkable feature of water-based magnetic liquids is their tendency to agglomerate when placed in a magnetic field. The aggregation can be so severe as to destabilise the colloid and produce sedimentation. Krueger (1980) describes experiments in which agglomerates ranging in size from a few particles to as many as 10^{10} particles can be detected. At a microscopic level the transmission electron microscope has demonstrated the existence of chains formed by ferrofluid dried in the presence of a magnetic field (Goldberg *et al* 1971). In this case the chains are 3–4 particles in width. We shall refer to chains of these dimensions (or smaller) as microchains. Obviously the smallest microchain is a dimer. Theoretical work on particle chaining at this level was initiated by de Gennes and Pincus (1970). More recently, Chantrell *et al* (1980) using Monte Carlo methods, have investigated the behaviour of field-induced chains.

On the other hand Hayes (1975) followed the *in situ* formation of chains in water-based ferrofluids using optical microscopy. The chains increased in size as a function of time and ultimately assumed large proportions—at least compared with those observed with the electron microscope. Hereafter chains of dimensions visible in the optical microscope at fairly low magnification will be referred to as macrochains. This paper reports an extension to the method of Hayes which allows a more sensitive detection of local inhomogeneities in optical properties (and their correlation with chain formation). It is important to note that such information may not normally be accessible to techniques which monitor the bulk optical anisotropy.

0022-3727/85/071281 + 10 $02.25

2. Experimental procedure

The studies were carried out with a four year old water-based (A05) Fe_3O_4 magnetic liquid of nominal magnetisation 200 G as supplied by Ferrofluidics Corporation. Macrochain formation was studied as a function of time in the as-received liquid as well as samples diluted five-fold by volume (i.e. 5 volumes of deionised water to 1 volume of initial fluid, hereafter designated as 5/1).

The ferrofluid was mounted for examination in a cylindrical glass cell 9 mm in diameter and 400 μm in height. The liquid was introduced via a syringe prior to sealing with a glass cover smeared with a thin film of vacuum grease: under these conditions the trapped fluid could survive indefinitely without evaporation. Thereafter the cell was placed between the poles of a specially constructed electromagnet (maximum field of 2.4×10^4 A m^{-1}) which fitted directly on the specimen stage of the microscope. Due to the finite thickness of the cell base, the maximum objective magnification available was $\times 16$.

All the observations were made with a Reichert MEFII polarising microscope fitted with a transmission light stage. A quarter-wave plate (calibrated for sodium 589 nm light) was inserted between specimen and analyser (see figure 1). The plate together

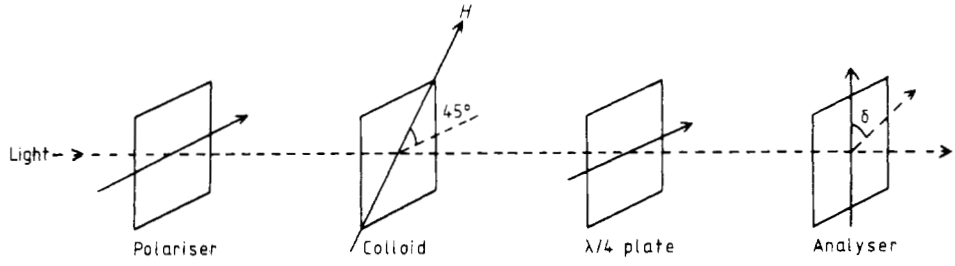

Figure 1. Disposition of principal optical components.

with the rotatable analyser constitute the de Sénarmont compensator, a device used extensively for the measurement of relative phase retardation of thin crystalline sections. The microscope was set up following standard procedure (Hartshorne and Stuart 1960) with (i) crossed polars (ii) the slow or fast axis of the quarter-wave plate parallel to the analyser and (iii) the magnetic field direction (which defines the slow axis in the colloid) aligned at 45° to the polariser axis. The operation of the compensator may be understood as follows.

The colloid layer is optically equivalent to a uniaxial crystal (Hartshorne and Stuart 1960) with two principal refractive indices corresponding to the fast and slow axes. (The latter directions are assumed invariant throughout the fluid including the macrochains.) Upon entering the colloid, linearly polarised light of unit amplitude splits into waves vibrating in two planes. One plane contains the propagation direction and the external field (parallel to the slow axis); the other plane is perpendicular and contains the fast axis. Their respective amplitudes are

$$\frac{s}{\sqrt{2}} \sin \omega t \qquad \frac{r}{\sqrt{2}} \sin(\omega t + \varphi)$$

where $\varphi = 2\pi\Delta n d/\lambda$ is the relative phase difference introduced between the two waves. Δn and d are the birefringence and thickness of the colloid layer respectively. r and s ($0 \leqslant r, s, \leqslant 1$) are dichroic factors which represent the unequal absorption of light along the fast and slow axes of the colloid. λ is the wavelength of light.

After passing through the quarter-wave plate (see figure 1) whose fast axis is assumed to lie parallel to the transmission azimuth of the initial polarised beam, the resulting vibrations have amplitudes

$$a_F = (s/2)\sin[\omega t + (\pi/2)] + (r/2)\sin[\omega t + \varphi + (\pi/2)]$$
$$a_s = (s/2)\sin\omega t - (r/2)\sin(\omega t + \varphi).$$

If the analyser is now allowed to rotate through an angle δ from its initial crossed position ($\delta = 0$), all other components remaining fixed, the resultant amplitude passing into the eyepiece of the microscope is given by

$$A = a_F \sin\delta + a_s \cos\delta.$$

After substitution for a_F and a_s and taking into account the phase difference between the waves it may easily be shown that the relative intensity, I, transmitted by the analyser is

$$I = \tfrac{1}{4}[r^2 + s^2 - 2rs\cos(2\delta - \varphi)]. \tag{1}$$

This equation is the basis of the classical de Sénarmont technique. If the analyser is rotated away from the crossed position in the correct sense a critical value of δ ($=\delta_e$) is reached for which the transmitted intensity is a minimum. This occurs when

$$\delta = \delta_e = \varphi/2 = \pi\Delta n d/\lambda. \tag{2}$$

We shall refer to δ_e as the extinction angle. In the absence of dichroism (i.e. when $r = s$) the minimum is zero. Of course $I = 0$ when $r = s = 0$ (regardless of δ) as this corresponds to complete absorption. It was noted in practice that the extinction angle using white light was—within experimental error—identical to that found using sodium light. The monochromatic source was therefore dispensed with, the unfiltered white light having a greater intensity.

The compensator may also give a measurement of dichroism (r/s) provided the quarter-wave plate is rotatable (see Goldstein 1970). If dichroism is present a more pronounced minimum than that predicted on the basis of equation (1) can be found by setting the wave plate and analyser to new independent values. (Note that equation (1) is derived under the condition that the principal axes of the quarter-wave plate are fixed parallel to the initially crossed polars.) Our quarter-wave plate was rotatable but no greater extinction could be found and it is therefore concluded that dichroism is negligible for the colloid thickness and applied fields used in these experiments.

In principle, once d is known, the bulk birefringence, $\overline{\Delta n}$ of the specimen may be determined by measurement of the extinction angle (equation (2)). Unfortunately the judgement of this angle is not easy, being hindered by the formation of macrochains which make the field of view non-uniform (figures 2–4). It would appear that the eye has greater acuity for discerning changes in intensity levels of a uniform field of view. However it was possible to divert the light to a photocell and thereby observe the minimum electronically. The optical properties of individual chains were monitored by taking a sequence of photographs at analyser settings differing by intervals of 0.5°.

3. Results

Figure 2 shows photographs of undiluted ferrofluid in polarised light but with the quarter-wave plate removed. They illustrate well the phenomenon reported by Hayes (1975) of chaining induced by an external field, in this case 3×10^3 A m^{-1}. The macrochains, several hundred micrometres in length and running parallel to the field direction, are remarkable for their uniformity. Figure 2(*b*) was taken some 7 min after application of

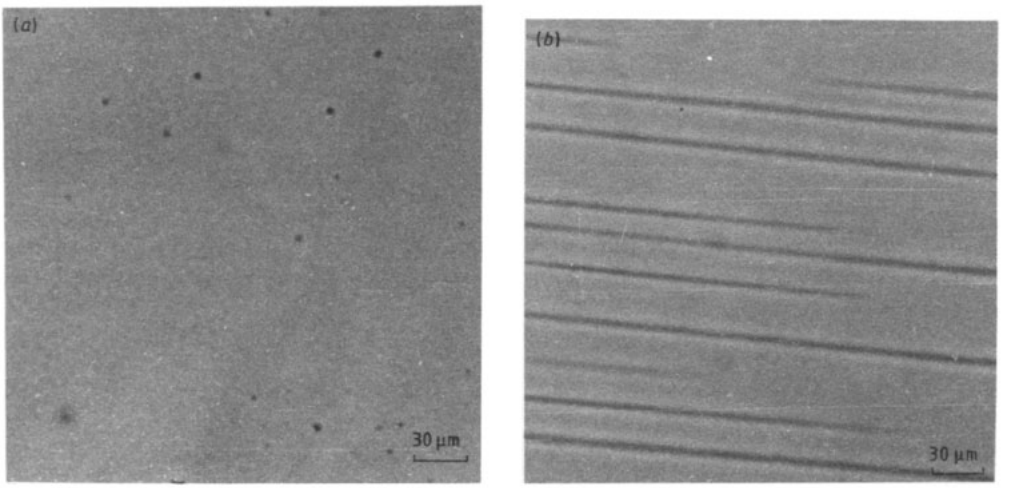

Figure 2. Macrochain formation in as-received colloid (*a*) before and (*b*) 7 min after switching on magnetic field of 3×10^3 A m^{-1}; observed in polarised light.

the field. By using a simple area counting technique and assuming that the macrochains where cylinders with a circular cross-section it was estimated that the volume fraction of total liquid contributing to macrochains was ~0.06.

That the chains are revealed at all indicates that they possess optical properties different from the surrounding fluid. In fact they are visible even in unpolarised light but are much more contrasted when a quarter-wave plate is inserted into the system. These points are demonstrated in figure 3 which shows macrochain formation in a 5/1 diluted ferrofluid after exposure to a field of 8×10^3 A m^{-1} for (*a*) 34 min and (*b*) 36 min. Unlike figure 2 the fluid here had been cycled several times previously in a magnetic field: for some reason this tends to promote the growth of irregular chains (i.e. of different widths). To facilitate a description of the results, chain contrast will be defined as

$$C = \frac{I_{ch} - I_l}{I_{ch} + I_l} \tag{3}$$

where I_{ch} and I_l are the intensities observed in the chain and surrounding liquid respectively. Since figure 3(*a*) was taken in unpolarised light the negative contrast indicates that the chains have a higher absorption vis à vis the surrounding liquid.

The effect on chain contrast of changing the angular setting δ, of the analyser, is illustrated in figure 4 which is a sequence of photographs (chosen from a longer series)

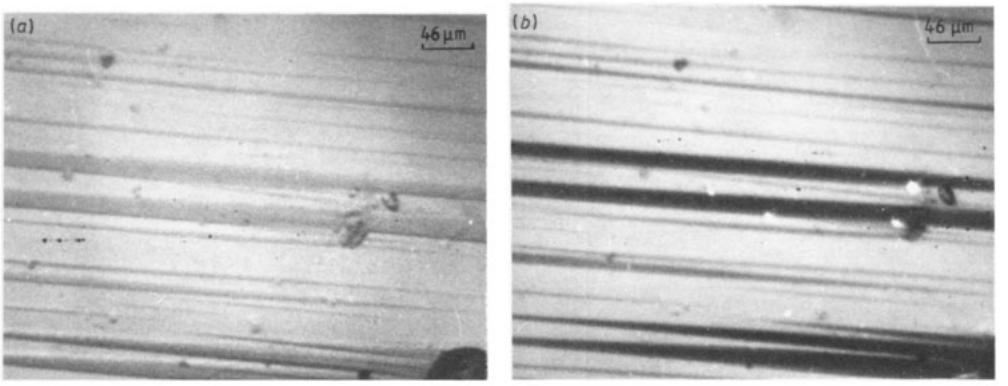

Figure 3. Macrochains in 5/1 diluted colloid in a field of 8×10^3 A m^{-1}, after 34 min: (*a*) observed in unpolarised light and (*b*) same area observed in polarised light with quarter-wave plate inserted.

of a 5/1 fluid sample. All the photographs were taken within a time interval of about 6 min some 30 min after the application of a 3×10^3 A m^{-1} field and by which time the geometrical disposition of the macrochains was sensibly constant. The volume fraction occupied by chains was estimated at 0.04. The most striking feature of figure 4 is the reversal of contrast observed for all macrochains with respect to the surrounding fluid. At some critical value, δ_0, the chain contrast is zero but careful scrutiny of the original

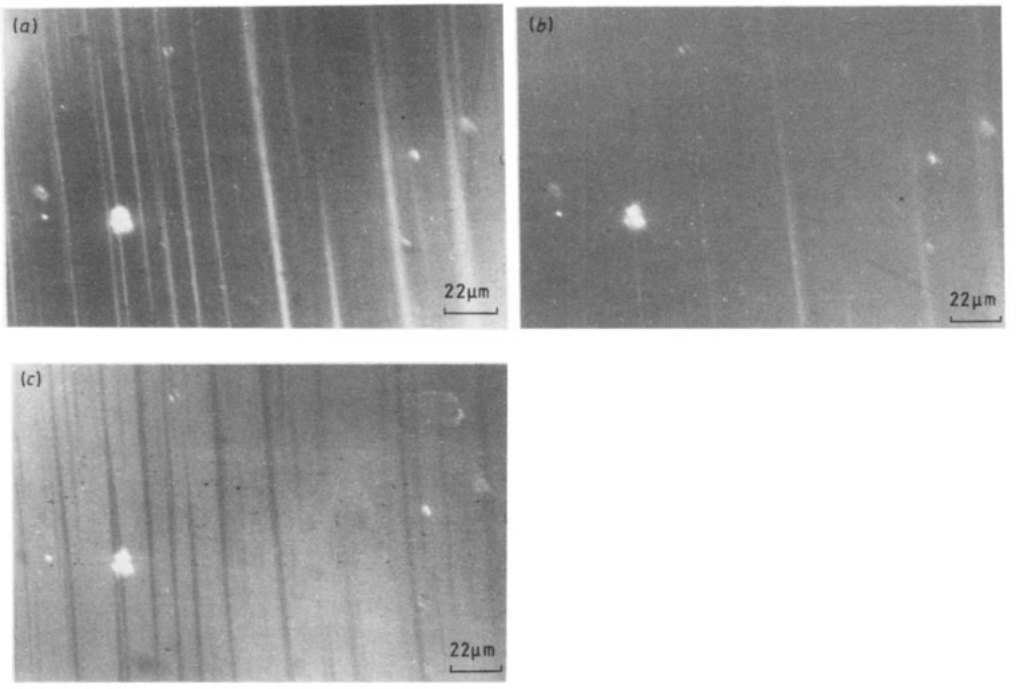

Figure 4. Macrochains formed in 5/1 diluted colloid after 30 min in a field of 3×10^3 A m^{-1}, showing effect of changing analyser setting, δ, from initial crossed position. All observations taken in polarised light with quarter-wave plate inserted. δ = (*a*) 41° (*b*) 46° (*c*) 50°.

negatives shows that not all chains 'disappear' at the same setting of δ_0; indeed it is possible to find negative and positive contrast chains simultaneously over a narrow range (~3°) of analyser settings. As a rule the wider a chain the greater the critical angle, δ_0, at which C becomes zero.

Particular significance is attached to δ_0 because in practice it is the parameter that can be best judged by the eye. This is to be contrasted with the true extinction angle δ_e for an individual macrochain which cannot normally be detected because of the noisy background of the images. Figure 4(*b*) is also significant because for this analyser setting (46°) and notwithstanding the variations due to macrochains the eye perceived the overall intensity of the layer to be a minimum. In fact the photocell recorded a minimum intensity at the identical setting of $\bar{\delta}_e = 46°$. The implication is that the layer in focus is typical of the whole sample and so $\bar{\delta}_e = 46°$ may be taken as a reliable figure for determining the birefringence of the bulk fluid. This quantity will be denoted Δn. It is important to note that whether recorded visually or with the photocell, the value of $\bar{\delta}_e$ remained constant to within 4% over a 2 h period: this despite the obvious changes taking place within the fluid specimen. The essential invariance of Δn will play a role in establishing a model for interpreting the data.

Although the addition of the quarter-wave plate enhances contrast it is unfortunate that quantitative measurements of the optical properties of individual macrochains are close to the limit of sensitivity of the compensator. Careful scrutiny of the negatives shows that $\delta_0 - \bar{\delta}_e \sim 0.5°$ for a typical chain width of 4 μm. (For smaller diameter chains $\delta_0 - \bar{\delta}_e$ is not measurable.) The largest discrete chain, of diameter 7 μm, had $\delta_0 - \bar{\delta}_e \sim 1°$.

It will be shown below that a determination of $\delta_0 - \bar{\delta}_e$ can lead to a rough estimate of macrochain birefringence.

4. Discussion

Although the optical microscope demonstrates the existence of macrochains it must not be inferred that the intervening, apparently unchained fluid, is passive or neutral. Indeed the opposite is true. It is known that the mechanism responsible for induced birefringence is established throughout the fluid almost instantaneously, i.e. before chains are observed in the microscope. Furthermore it is likely that the intervening fluid does in fact contain microchains as well as dimers and trimers. The existence of microchains has been postulated as the origin of the anomalously high birefringence and dichroism observed in water-based ferrofluids (Scholten 1980).

It is obvious that the optical properties of macrochains are somewhat different from the surrounding fluid, e.g. their greater absorption of unpolarised light. Hayes (1975) has shown that the formation of macrochains affects the scattering property of ferrofluid, a phenomenon related to changes in the magneto-optical extinction coefficients (Mehta 1983). These changes reflect a departure from classical Rayleigh scattering. It would not therefore be surprising to find that the birefringence of macrochains is also different from that of disperse liquid. The experimental results presented above lead to the same conclusion as may be seen from the following semi-quantitative argument.

Consider two adjacent optical paths, one comprising a macrochain and the other an identical distance of 'unchained' fluid. If the birefringence of chained fluid Δn_{ch} is greater than the birefringence of unchained liquid, Δn_l, then the phase retardations are such that $\varphi_{ch} > \varphi_l$. Assuming that dichroism and absorption are negligible ($r = s = 1$) equation (1)

becomes

$$I = \sin^2[\delta - (\varphi/2)]. \tag{4}$$

Equation (4) is plotted in figure 5 for two arbitrary values of φ but subject to the condition that $\varphi_{ch} > \varphi_l$. The properties of chain contrast predicted on the basis of figure 5 are broadly consistent with the experimentally observed results. On the other hand, dichroism alone cannot account for the results—as may be verified by analysis of equations (1) and (3) subject to the condition that $\varphi_{ch} = \varphi_l = 0$. Regardless of the values of r and s, it is impossible to obtain a change in the sign of C as δ is varied.

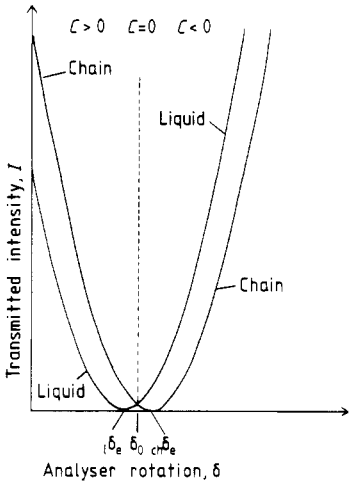

Figure 5. A plot of equation (4) for arbitrary values of φ_{ch} (chain) and φ_l (liquid) to predict chain contrasts as a function of analyser setting. Note that $C = 0$ for $\delta = \delta_0$. $_l\delta_e$ and $_{ch}\delta_e$ are the extinction angles for liquid and chain respectively.

It may be concluded that the enhanced birefringence of macrochains is the principal mechanism responsible for contrast in the microscope but the magnitude of the difference is not easy to deduce from the data. This is because, for a given setting of the microscope, the contrast changes observed are restricted to a horizontal layer whose thickness is of the order of the depth of field, estimated as 10 μm for the objective used. Features above and below this layer are blurred. On the contrary, the state of the polarised light entering the analyser is determined by an optical path through the whole cell. The problem is therefore one of deducing information about a two-dimensional layer (seen in the eyepiece of the microscope) from optical data integrated through the thickness of the colloid layer. This may only be resolved by devising a reasonable model of the colloidal suspension.

The model is illustrated in figure 6. Apart from the layer of thickness t, in focus, the fluid is assumed to possess the (invariant) bulk birefringence $\overline{\Delta n}$. Within the layer the macrochains are characterised by birefringence Δn_{ch} which is independent of chain dimensions while the surrounding liquid has birefringence Δn_l. The chains are taken to be cylindrical with constant circular cross-section. Although no mechanism for the birefringence of macrochains need be postulated its independence of chain dimension is justified on the basis of two reasonable assumptions. First, the packing of individual

aggregated particles within macrochains is constant as chains form: moreover this is higher than the neighbouring particle concentration as evidenced by the increased absorption. Second, the effective shape-dependent depolarisation factors (and hence optical polarisabilities) are essentially constant once the chains assume an aspect ratio greater than 10:1 (acquired very early in the growth process). Both packing and shape are likely to influence birefringence so that if these parameters are independent of macrochain dimension, it is probable that birefringence will be also.

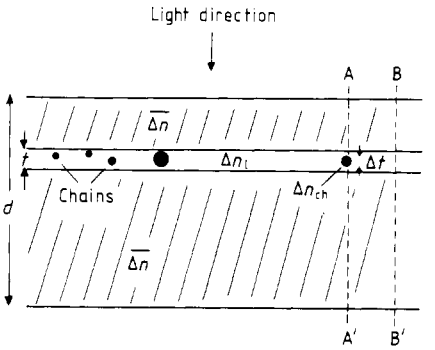

Figure 6. Proposed model for calculation of chain birefringence. d, t and Δt are dimensions of total colloid layer, layer in focus and macrochains respectively.

Of course as macrochaining proceeds, particles are drawn from the remaining liquid which thereby becomes less concentrated thus leading to a diminution in Δn_l. A functional relationship between Δn_l and Δn_{ch} may be derived on the basis that the bulk birefringence, $\overline{\Delta n}$ of the sample remains unchanged. The relation is

$$\overline{\Delta n} = \Delta n_l(1 - \omega) + \omega \Delta n_{ch} \tag{5}$$

or

$$\Delta n_l = \frac{\overline{\Delta n} - \omega \Delta n_{ch}}{1 - \omega} \tag{6}$$

where ω is the fractional volume of the sample contained within macrochains. Equations (5 and 6) are valid for $0 < \omega < \omega_c$ with $\omega_c = \overline{\Delta n}/\Delta n_{ch}$. Experimentally observed values of ω (see above) are at the lower end of the range. This relationship is derived on the likely assumption that the birefringence of the liquid, Δn_l, is linearly related to the volume fraction of particles remaining in the 'unchained' fluid.

The contrast between a chain and neighbouring fluid is obtained by considering two adjacent light paths one of which contains a macrochain. (It is assumed that no more than one macrochain is traversed by a given light beam as it passes through the layer in focus.) Under these conditions it may be shown (see appendix) that a macrochain has zero contrast when

$$(\delta_0 - \bar{\delta}_e) = \frac{\pi}{2\lambda} \frac{\Delta t - 2t\omega}{1 - \omega} (\Delta n_{ch} - \overline{\Delta n}). \tag{7}$$

This relation enables an estimate of $\Delta n_{ch} - \overline{\Delta n}$, to be made in terms of the most easily measured quantities, namely $\delta_0 - \bar{\delta}_e$. As expected equation (7) shows that $\delta_0 - \bar{\delta}_e$

depends on chain width. Substituting $\omega = 0.04$, $t = 10\ \mu m$, $\lambda = 0.5\ \mu m$, then for a chain width of 4 μm and an observed $\delta_0 - \bar{\delta}_e$ of 0.5° we have $\Delta n_{ch} - \overline{\Delta n} = 83 \times 10^{-5}$. Similarly for a chain width of 7 μm and $\delta_0 - \bar{\delta}_e = 1°$ we get $\Delta n_{ch} - \overline{\Delta n} = 86 \times 10^{-5}$. Since $\overline{\Delta n} = \lambda/\pi d\bar{\delta}_e = 32 \times 10^{-5}$ we have $\Delta n_{ch} \sim 115 \times 10^{-5}$ or some four times greater than the original fluid birefringence. This seems a not unreasonable result and one that could be accounted for in terms of an increased packing of particles within the macrochain aggregates. However this may not be the sole mechanism responsible for elevated chain birefringence. A value of $t = 20\ \mu m$ does not change the predicted results by much. Perhaps of more significance is the fact that dichroism has been ignored in the derivation of equation (7). Whilst this does not affect the observed value of $\bar{\delta}_e$ it would influence the observed value of δ_0. Unfortunately the polarising microscope does not provide an experimental value of dichroism. Either the dichroism is negligible or the microscope is not sufficiently sensitive. However, the argument adduced above proving that the general nature of the contrast must be attributed to birefringence should not be forgotten.

5. Conclusions

It has been demonstrated that the contrast of macrochains in water-based ferrofluids can be considerably enhanced by the addition of a quarter-wave plate to the conventional polarising microscope. Moreover, the contrast changes observed as the analyser is rotated must be attributed to the macrochains possessing a locally increased optical birefringence. An estimate of the macrochain birefringence, ignoring the effect of dichroism, indicates a value of $\Delta n_{ch} = 115 \times 10^{-5}$ which is to be compared with the initial bulk birefringence of the (five-fold diluted) fluid of $\Delta n = 32 \times 10^{-5}$. It is possible that the enhanced birefringence may be attributable to a higher packing within the macrochains. The fact that the bulk birefringence scarcely alters during the aggregation process would support the view that local inhomogeneities in birefringence are the consequence of local redistribution of particles or previously existing microchains.

Acknowledgments

My thanks go to Dr R W Chantrell for his critical reading of the manuscript and to Miss S M Davies and Mr P J Keating who contributed to the experimental aspects of the work.

Appendix

The model is outlined schematically in figure 6. For light paths AA′ and BB′, the phase differences introduced by the colloid layer are

$$\varphi_{ch} = \frac{2\pi}{\lambda}[\Delta n_{ch}\Delta t + (t - \Delta t)\Delta n_l + (d - t)\overline{\Delta n}] \tag{A1}$$

and

$$\varphi_l = \frac{2\pi}{\lambda}[t\Delta n_l + (d - t)\overline{\Delta n}] \tag{A2}$$

respectively.

In the absence of dichroism the condition for zero chain contrast is given, from equations (3) and (4), by

$$\delta_0 = (\varphi_{ch} + \varphi_l)/4 \tag{A3}$$

whence, using equations (A1 and A2), we derive

$$\delta_0 = \frac{\pi}{2\lambda}[2(d-t)\overline{\Delta n} + 2t\Delta n_l + (\Delta n_l - \Delta n_{ch})\Delta t]. \tag{A4}$$

We now make use of equation (6) to eliminate Δn_l. Equation (A4) becomes

$$\delta_0 = \frac{\pi}{2\lambda(1-\omega)}[2d\overline{\Delta n}(1-\omega) + (\Delta n_{ch} - \overline{\Delta n})(\Delta t - 2\omega t)]. \tag{A5}$$

Rearranging equation (A5), we get

$$[2\lambda\delta_0(1-\omega)/\pi] - 2d\overline{\Delta n}(1-\omega) = (\Delta n_{ch} - \overline{\Delta n})(\Delta t - 2\omega t). \tag{A6}$$

But $\delta_{\bar{e}} = (\pi/\lambda)d\overline{\Delta n}$, the extinction angle for the bulk specimen. Substituting for $\overline{\Delta n}$ on the left-hand side of equation (A6) we have

$$\delta_0 - \bar{\delta}_e = (\pi/2\lambda)\frac{\Delta t - 2t\omega}{1-\omega}(\Delta n_{ch} - \overline{\Delta n}) \tag{A7}$$

which corresponds to equation (7) in the main text.

References

Chantrell R W, Bradbury A, Popplewell J and Charles S W 1980 *J. Phys. D: Appl. Phys.* **13** L119
de Gennes P G and Pincus P A 1970 *Phys. Kondens. Mat.* **11** 189
Goldberg P, Hansford J and van Heerden P J 1971 *J. Appl. Phys.* **42** 3874
Goldstein D J 1970 *J. Microsc.* **91** 19
Hartshorne N A and Stuart A 1960 *Crystals and the Polarising Microscope* (London: Edward Arnold)
Hayes C F 1975 *J. Colloid Interf. Sci.* **52** 239
Krueger D A 1980 *IEEE. Trans. Magn.* **MAG-16** 251
Majorana Q 1902 *Phys. Z.* **4** 145
Mehta R V 1983 *J. Magn. Magn. Mater.* **39** 64
Scholten P C 1980 *IEEE. Trans. Magn.* **MAG-16** 221